MedChemComm

ARTICLE

Design and synthesis of 5-aminolaevulinic Acid/3-hydroxypyridinone conjugates for photodynamic therapy: enhancement of protoporphyrin IX production and photo-toxicity in tumor cells

Received 00th January 20xx,
Accepted 00th January 20xx

DOI: 10.1039/x0xx00000x

www.rsc.org/

Tao Zhou[a]*, Le-Le Shao[a], Sinan Battah[b]*, Chun-Feng Zhu[a], Robert C. Hider[c], Brandon J. Reeder[b], Asma Jabeen[b], Alexander J. MacRobert[d], Gerui Ren[a], Xinle Liang[a]

5-Aminolaevulinic acid (ALA) and its derivatives have been widely used in photodynamic therapy (PDT) as precursors of the photosensitizer, protoporphyrin IX (PpIX) in dermatology and urology. However, ALA–PDT is limited by the low bioavailability of ALA due to the fact that ALA is poorly absorbed by cells by virtue of its zwitterionic nature at physiological pH. In order to improve the therapeutical effect and induce higher levels of PpIX, a series of ALA prodrugs were synthesized by the conjugation ALA to 3-hydroxypyridin-4-ones (HPO) iron chelator using an amino acid linkage via amide bonds. Pharmacokinetic studies indicated that one ALA–HPO conjugate significantly enhanced PpIX production in a range of tumor cell lines over above that caused by ALA alone or the co-administration of ALA and CP94 (1,2-diethyl-3-hydroxypyridin-4-one). The intracellular porphyrin fluorescence levels showed good correlation with cellular photo-toxicity following light exposure, suggesting the potential application of the ALA–HPO conjugates in photodynamic therapy.

1. Introduction

Photodynamic therapy (PDT), based on the activation of exogenously applied or endogenously formed photosensitizers by visible light in the presence of molecular oxygen, is a promising treatment strategy for malignant and non-malignant lesions. Upon exposure to light, a photosensitizer generates singlet oxygen and/or free radicals, which oxidize cellular macromolecules, leading to the damage of a variety of subcellular substrates (such as phospholipid membranes, nucleic acids, and proteins), resulting in cell death.[1-3]ALA has been widely used in PDT for the treatment of actinic keratosis, squamous cell carcinoma, and Bowen's disease, as well as cutaneous microbial infections such as acne, onychomycosis, and verrucae.[4-8] ALA-induced PDT can also be used as a diagnostic tool for the visualization of precancerous changes in the mucosae by fluorescence spectroscopy.[9,10] The main disadvantage of this therapy is that ALA is poorly absorbed by cells due to its high hydrophilicity, resulting in low bioavailability.[11] In order to overcome this drawback, numerous effforts have been made, which are mainly centred on the development of ALA prodrugs with more favorable lipid solubility, such as esters,[12,13] peptide derivatives.[14,15] According to the action mechanism, ALA is metabolized via the heme biosynthesis pathway to produce the fluorescent photosensitizer protoporphyrin IX (PpIX).[16,17] Ferrochelatase can catalyze the conversion of PpIX to light inactive heme, leading to a decrease in the therapeutical effect.[18] Thus, the activity of ferrochelatase is a key factor that influences the accumulation of PpIX in the cell.[19,20] Iron chelators can inhibit the activity of ferrochelatase by scavenging the intracellular labile iron pool. It has been demonstrated that ALA–PDT can be modulated in the presence of iron chelators such as EDTA,[21] and desferioxamine.[22-24] Several studies have also demonstrated that a combination of ALA and the membrane permeable iron chelator CP94 (1,2-diethyl-3-hydroxypyridin-4-one) in PDT is an effective technique to increase the efficacy of ALA-PDT within cells under both in vitro and in vivo conditions.[25–28] Previously, we reported that ALA–HPO conjugates, in which the ALA moiety was linked to a HPO moiety via an ester bond, significantly enhanced PpIX formation in cells of the human breast adenocarcinoma (MDA-MB-468), in comparison with ALA alone or with a combination of ALA with deferiprone (1,2-dimethyl-3-hydroxypyridin-4-one).[29] In the present study, a range of novel ALA–HPO conjugates with reasonable lipophilicity were synthesized. In these molecules, ALA methyl ester was linked to phenylalanine or leucine via a peptide bond, while the HPO moiety was coupled to amino group on phenylalanine or leucine. The ALA–HPO conjugates are anticipated to be hydrolyzed by peptidases and esterases in the cytosol of tumor cells, liberating free ALA. The PpIX fluorescence induced by these ALA–HPO conjugates in a range of human tumor cell lines and their photo-toxicity have been investigated.

[a] School of Food Science and Biotechnology, Zhejiang Gongshang University, Xiasha, Hangzhou, Zhejiang, 310018, P. R. China. E-mail: taozhou@zjgsu.edu.cn
[b] Biological Sciences Department, University of Essex, Wivenhoe Park CO4 3SQ, UK. E-mail: shbatt@essex.ac.uk.
[c] Division of Pharmaceutical Science, King's College London, Franklin-Wilkins Building, 150 Stamford Street, London, SE1 9NH, UK
[d] Medical Laser Centre, Division of Surgical Sciences, University College London, Charles Bell House, 67-73 Riding House Street, London W1W 7JE

† Electronic Supplementary Information (ESI) available: Synthetic procedures and characterization of the compounds. See DOI: 10.1039/x0xx00000x

2. Results and discussion

2.1. Chemistry

The synthetic route of benzyl protected 3-hydroxypyridinones containing a carboxyl group (**5**) using maltol (**1**) as a starting material is presented in Scheme 1. The benzylation of maltol with benzyl chloride provided **2** in 86% yield. Condensation of **2** with primary amines under basic conditions provided the 3-hydroxypyridinone derivatives **3** in good yield (84–90%), which underwent selective oxidation of the methyl group at the 2-position with selenium dioxide in acetic anhydride to give aldehyde **4** in 77-80% yield. Further oxidation of **4** in the presence of sodium hypochlorite and sulfonic acid provided the carboxylic acids **5** in reasonable yield (54-62%). Coupling reaction of **5** with L-amino acid esters was carried out in the presence of 2-(6-chloro-1H-benzotriazole-1-yl)-1,1,3,3-tetramethylaminiumhexafluorophosphate (HCTU), giving product **6** in moderate to good yield (68-81%) (Scheme 2). Compounds **6** were then hydrolyzed with lithium hydroxide to the corresponding carboxylic acids **7** in excellent yield (91-94%). Conjugation of **7** and methyl 5-aminolaevulinate was achieved in the presence of HCTU to give **8** (75-81% yield), which were subjected to hydrogenation to remove benzyl groups, generating ALA–HPO conjugates **Z01-Z10** in excellent yield (93-97%) (Scheme 2). All the compounds were fully characterized by ^{1}H NMR, ^{13}C NMR, MS and HRMS.

2.2. Fluorescence Pharmacokinetics

In order to assess the efficacy of the structural designed ALA–HPO conjugates **Z01–Z10**, at the onset of this study the ability of these ALA–HPO conjugates to generate the active, fluorescent photosensitizer PpIX was investigated by measuring the fluorescence intensity of the peak emission at 635 nm after incubation with a range of tumor cell lines, including A549 cell line (human lung carcinoma), MCF-7 cell lines (human breast adenocarcinoma), KB cell line (human mouth epidermal carcinoma cells), LNCap cell line (human prostate cells derived from metastatic site lymph node) and BPH-1 cell line (normal human prostate epithelial cells).

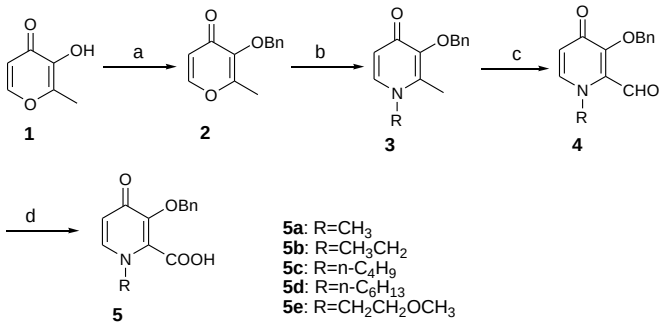

Scheme 1. Reagents and conditions：(a) BnCl, NaOH, CH_3OH, reflux, 7-8h; (b) RNH_2, NaOH, CH_3OH/H_2O, reflux, 2.5h; (c) SeO_2, $CH_3COOH/(CH_3CO)_2O$, reflux; (d) NH_2SO_3H, $NaClO_2$, acetone/H_2O.

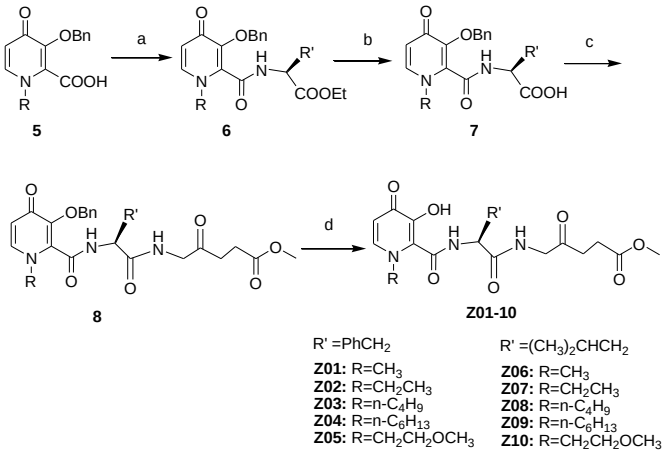

Scheme 2.Reagents and conditions： (a) HCTU, Et_3N, DMF, overnight; (b) i) LiOH, ii) Amberlite IR-120 (H form) ion exchange resin; (c) HCTU, Et_3N, DMF, overnight; (d) CH_3OH, Pd/C, 3h.

Firstly, the efficacy of **Z01–Z10** to produce PpIX in A549, KB, LNCap and BPH-1 cell lines at a concentration of 100 μM was assess by comparison with ALA (Fig. 1). It was found that after incubation for 24h, compounds **Z02–Z10** at this concentration did not markedly enhance the synthesis of PpIX in these cells as compared to ALA, some of them even led to the production of less PpIX than ALA. However, compound **Z01** was found to significantly increase PpIX production at 100 μM in A549, KB and LNCap cell lines, generating PpIX by 3.1, 2.9 and 4.0 times higher than that induced by ALA, respectively. For the BPH-1 cell line, the fluorescence intensity of PpIX induced by **Z01** was only 1.5 time larger than that induced by ALA, indicating that PpIX producing rate via heme biosynthesis pathway in tumor cell is much higher than that in normal cell. Significant differences of PpIX production was observed in these cell lines ($P < 0.05$). After incubation with **Z01**, the highest level of PpIX was detected in KB cell, the next in A549 cell. This difference could be attributed to the different peptidase and/or esterase bioavailability and activity in these cell lines, resulting in different releasing rates of free ALA.

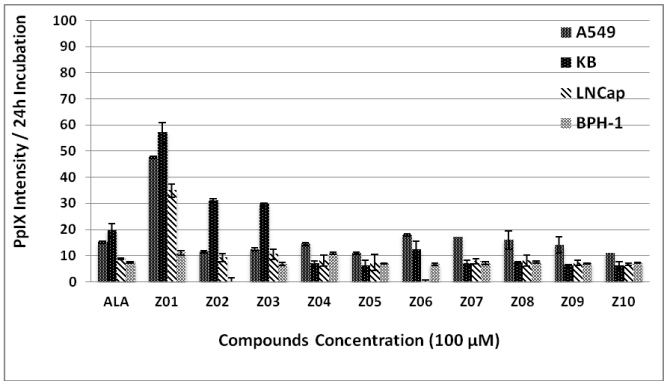

Fig. 1. PpIX production in A549, KB, LNCap and BPH-1 cell lines after incubation with 100 μM of ALA or ALA-HPO conjugates for 24 h at 37 °C and humidified by 5% CO_2. Bars represent standard deviation (n = 3).

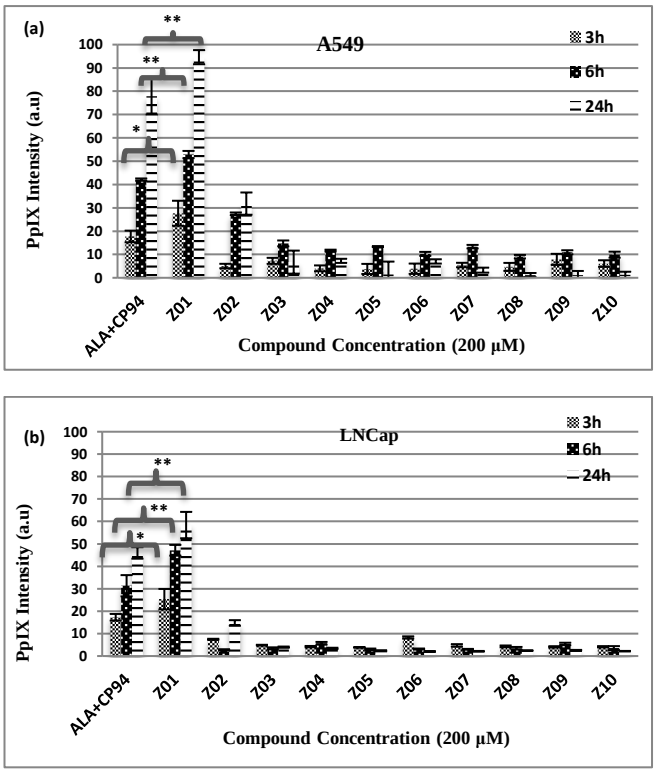

Fig. 2. PpIX fluorescence intensities produced after incubation in tumor cell lines with 200 µM of ALA–HPO conjugates, co-administration of ALA and CP94 (both 200 µM) for 3, 6 and 24 h at 37 °C and humidified by 5% CO_2. (a) incubation with A549 cell line; (b) incubation with LNCap cell line. Bars represent standard deviation (n=3). *represents a significant difference ($P < 0.05$), **represents a very significant difference ($P < 0.001$).

In this investigation, the efficacy of compounds **Z01–Z10** to produce PpIX in A549, LNCap, KB and PBH-1 cell lines was compared with co-administration of ALA and CP94 by a time-course study. In all the four cell lines, compounds **Z02–Z10** were less efficient than the co-administration of ALA and CP94 to produce PpIX. However, **Z01** was found to significantly enhance the PpIX production in comparison with the combination of ALA with CP94. It was found that PpIX fluorescence intensity profile of A549 cell line was similar to that of KB cell line at 200 µM at all incubation times. Thus, only the results of A549 cell line were presented (Fig. 2a). After incubation with the A549 cell line for 3, 6 and 24h, PpIX fluorescence intensities generated by **Z01** (200 µM) was determined to be 27.7, 52.9 and 94.6 a.u., respectively, which were 1.6, 1.3 and 1.2 times higher than those induced by ALA in combination with CP94 (17.7, 42.1 and 77.8 a.u. respectively). In the case of the LNCap cell line, after incubation for 3, 6 and 24h, PpIX fluorescence intensities generated by **Z01** (200 µM) was determined to be 25.3, 47.1 and 58.4 a.u., respectively; whereas those induced by ALA in combination with CP94 were 17.3, 31.3 and 46.0 a.u., respectively (Fig. 2b). The normal cell line PBH-1 produced a lower PpIX level than that presented for LNCap in Fig. 2b (data not shown). It is surprising that most of the newly synthesized ALA-HPO derivatives showed a similar efficacy in intracellular PpIX production to that of ALA with the exception of **Z01**. The lack of efficacy of generating PpIX from compounds **Z02**-**Z10** could partially be owing to their bioavailability within the cell lines under investigation. It was clearly noticeable some aggregation of those compounds on the surface of the incubated cells. Probably, the use of serum free media (in order to avoid releasing PpIX from the cells) containing the compounds would not promote the solubility of the lipophilic compounds, subsequently decreasing the intercellular availability. It was reported that the aggregation problem with the lipophilic compounds which led to reduction of uptake, was much less appreciable in full media with serum.[30] The calculated partition coefficient (ClogP) value[31] of **Z01** was -1.23, while the values of **Z02-Z10** range from -1.40 to 1.22, indicating that the lipophilicities of all these ALA-HPO conjugates were increased as compared to ALA (ClogP -3.91). However, it has been previously reported that increasing the lipophilicity of ALA derivatives to certain level could negatively influence the uptake of the compound.[32,33] As this compound series were all expected to penetrate the cell membrane by a passive diffusion mechanism, it is reasonable to assume that the relatively poor performance of derivatives (**Z02-Z10**) in terms of PpIX production also reflects a slower rate of metabolism and a corresponding lower affinity for the peptidases and/or esterases involved in the release of ALA from the prodrug. The superior activity of **Z01** to the other derivatives was probably due to its higher intercellular bioavailability and its more rapid metabolism of the prodrug.

Owing to aggregation problem, we wished to evaluate the potential of **Z01** in more cell lines. KB was known to be

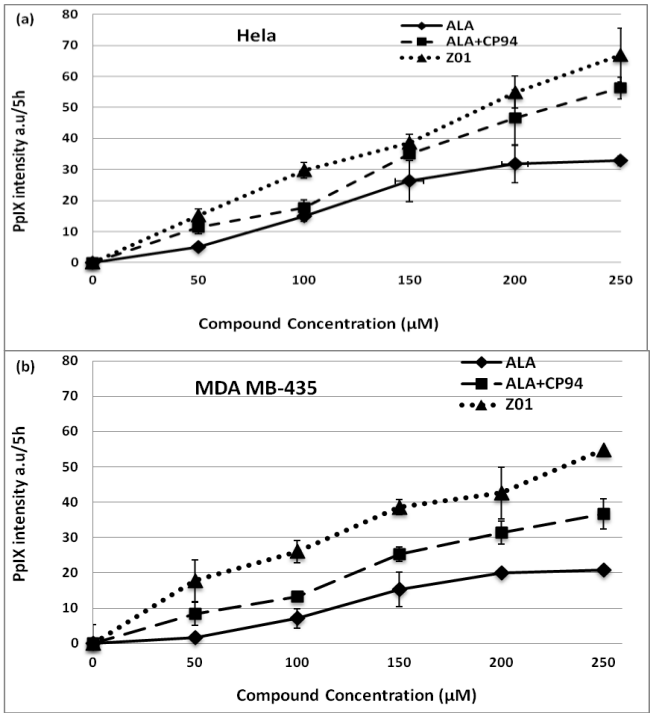

Fig. 3. Kinetics of PpIX fluorescence in (a) Hela cell line; (b) MDA MB-435 cell line. Fluorescence measurements after incubation with variable concentration (50–250 µM) of ALA, ALA in combination with CP94, and **Z01** for 5h at 37 °C humidified by 5% CO_2. Bars represent standard deviation (n=3). ($P < 0.001$ to 0.05).

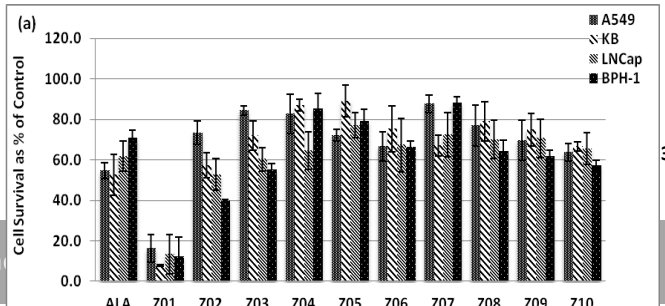

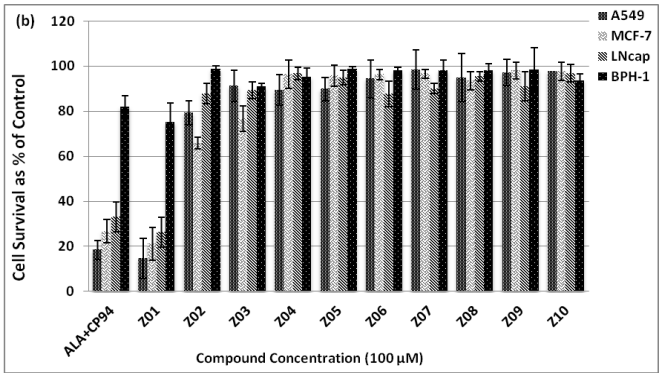

Fig. 4. Photo-toxicity after incubation with ALA or ALA+CP94, and ALA-HPO conjugates in a range of cell lines assessed by MTT assay. Cells were incubated with the compounds for 4 h and irradiated with blue light (2.5 J·cm^{-2}). (a) compound concentration 200µM; (b) compound concentration 100µM.

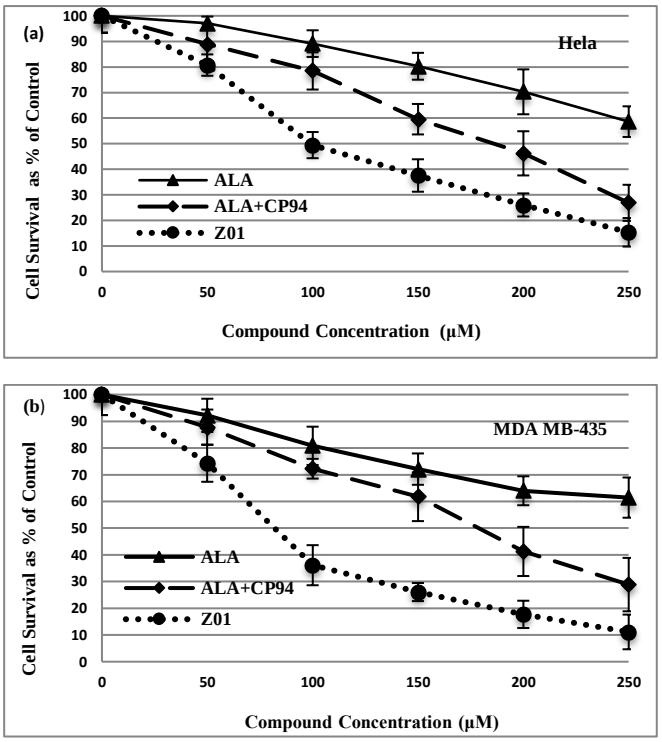

Figure 5. Photo-toxicity after incubation with ALA, ALA+CP94 and **Z01** in tumor cell lines assessed by MTT assay. Cells were incubated with the compounds for 4 h and irradiated with blue light (2.5 J·cm^{-2}).(a) Hela cell line; (b) MDAMB-435 cell line.

contaminated by Hela in all the stocks worldwide.[34] Thus, Hela cell line (human cervical cells) and MDA-MB 435 cell line (breast cancer cells) were selected in the evaluation. As shown in Fig. 3, compound **Z01** exhibited a dose dependent response of PpIX production at concentrations ranging between 50–250 µM in both Hela and MDA MB-435 cell lines. Again, **Z01** was more efficient in PpIX production in these two cell lines than co-administration of ALA and CP94, which was found to enhance PpIX levels when compared to ALA alone (P<0.001 to 0.05).

2.3. Cytotoxicity

The photo-toxicity of prodrugs **Z01-Z10** (cells incubated with the compounds and exposed to blue light) on the A549, KB, LNCap, BPH-1 and MCF-7 cell lines was investigated (Fig. 4). The percentage of cell survival with respect to the control cells (without compounds) was calculated for the investigated compounds. After the incubation of the tumor cells with 200 µM of **Z01**, followed by the irradiation with blue light, efficient cell killing was observed. The survival percentages of A549, KB, LNCap and BPH-1 cell lines treated **Z01** were determined to be 16.3, 7.8, 13.5 and 12.4%, respectively; those data in the case of ALA were 54.7, 52.6, 61.9 and 70.8%, respectively (Fig. 4a). However, overall cytotoxicity of **Z02-Z10** was not found to be significantly enhanced as compared to ALA (Fig. 4a). These results were in agreement with those obtained from PpIX fluorescence experiments. The comparison of cytotoxicity of **Z01-Z10** with co-administration of ALA and CP94 was also investigated at both 100 µM (Fig. 4b) and 200 µM (data not shown). At a concentration of 100 µM, **Z01** was found to be more efficient in cell killing than the combination of the ALA with CP94 (P < 0.05). The survival percentages of A549, MCF-7, LNCap and BPH-1 cell lines treated with **Z01** were determined to be 14.7, 21.1, 26.3 and 75.1%, respectively; those data in the case of ALA combined with CP94 were 18.4, 26.7, 33.1 and 81.9%, respectively (Fig. 4b). Thus, at this concentration, both **Z01** and ALA in combination with CP94 were found to be much less toxic on normal cells than on tumor cells. At 100 µM, compounds **Z02-Z10** were all found to be of low toxicity to the tested tumor cell lines.

The photo-toxicity of the most active conjugate **Z01** on additional two cell lines (Hela and MDA MB-435) in comparison with ALA, and ALA+CP94 over a range of concentrations between 50-250 µM is presented in Fig. 5. The cytotoxicity was dose dependent. It was found that **Z01** exhibited the highest photo-toxicity, and ALA the lowest, on these two cell lines. Significant differences between the treatments were observed (P < 0.05). The survival percentages of Hela cell line treated with **Z01**, ALA and ALA+CP94 at 250 µM were determined to be 15.3, 58.6 and 26.9% respectively. For MDA MB-435 cell line incubated with **Z01** and ALA (250 µM), the survival percentages were 11.1, 61.4 and 28.9%, respectively.

The "dark" toxicity of the ALA-HPO conjugates **Z01-Z10** (cells incubated with the compounds without light exposure) on A549, MCF-7, LNCap and BPH-1 cell lines as percentages of control (cells without compounds and without light exposure) was evaluated. The data indicated that there was no significant toxicity found for ALA or all the investigated compounds at 200 µM after 4h incubation (data not shown).

3. Experimental

The general synthetic procedures and spectral data for allcompounds are given in the ESI.† The spectral data for the final compounds **Z01-10** are given below.

3.1. Spectral data for compounds Z01-10

Z01. ^{1}H NMR (DMSO-d_6, 500MHz) δ 2.50 (t, J=6.5Hz, 2H, CH_2COO), 2.70 (t, *J*=6.5Hz, 2H, $COCH_2$), 2.87 and 3.17 (m, 2H, CH_2), 3.54 (s, 3H, $COOCH_3$), 3.58 (s, 3H, NCH_3), 3.97-4.08(m, 2H, CH_2CO), 4.87-4.92 (m, 1H, CH), 7.18-7.36 (m, 6H, Ph and buried C5-H in pyridinone), 8.14 (d, *J*=7.5Hz, 1H, C6-H in pyridinone), 8.70 (t, *J*= 5.5Hz, 1H, NH), 9.51 (d, *J*=8.5Hz, 1H, NH).^{13}C NMR (DMSO-d_6, 125MHz) δ 27.1, 33.9, 37.5, 42.8, 48.4, 51.4, 53.9, 111.7, 126.5, 128.2, 129.3, 136.3, 137.3, 138.9, 142.9, 158.9, 161.7, 170.6, 172.6, 205.1. ESI-MS: *m/z* 444 ($[M+H]^+$). HRMS-ESI: calcd. for $C_{22}H_{26}N_3O_7$ 444.1771 ($[M+H]^+$), found 444.1762.

Z02. ^{1}HNMR (DMSO-d_6, 500MHz) δ 1.13 (t, *J*=7.0Hz, 3H, CH_3), 2.50 (t, *J*=6.5Hz, 2H, CH_2COO), 2.71(t, *J*=6.5Hz, 2H, $COCH_2$), 2.87 and 3.19 (m, 2H, CH_2), 3.57 (s, 3H, $COOCH_3$), 3.73 and 3.97 (m, 2H, CH_2CO), 4.02 (q, *J*= 7.0Hz, 2H, NCH_2), 4.93 (m, 1H, CH), 7.20-7.36 (m, 5H, Ph), 7.42 (d, *J*=7.0Hz, 1H, C5-H in pyridinone), 8.26 (d, *J*=7.0Hz, 1H, C6-H in pyridinone), 8.72 (t, *J*=5.5Hz, 1H, NH), 9.60 (d, *J*=8.5Hz, 1H, NH). ^{13}C NMR (DMSO-d_6, 125MHz) δ 16.3, 27.1, 33.8, 37.5, 48.4, 51.4, 51.5, 54.1, 112.3, 126.5, 128.2, 129.2, 136.3, 137.3, 137.6, 142.8, 158.9, 161.4, 170.6, 172.6, 205.1. ESI-MS: *m/z* 458 ($[M+H]^+$). HRMS-ESI: calcd. for $C_{23}H_{28}N_3O_7$ 458.1927 ($[M+H]^+$), found 458.1924.

Z03. 1H NMR (DMSO-d_6, 500MHz) δ 0.75 (t, *J*=7.5Hz, 3H, CH_3), 1.05 (m, 2H, CH_2), 1.52 (m, 2H, CH_2), 2.49 (t, *J*=6.5Hz, 2H, CH_2COO), 2.70 (t, *J*=6.5Hz, 2H, $COCH_2$), 2.87 and 3.17 (m, 2H, CH_2), 3.57 (s, 3H, $COOCH_3$), 3.69 and 4.06 (m, 2H, CH_2CO), 4.01 (t, *J*=5.5Hz, 2H, NCH_2), 4.86 (m, 1H, CH), 7.19-7.39 (m, 6H, Ph and buried C5-H in pyridinone), 8.24 (d, *J*=7.0Hz, 1H, C6-H in pyridinone), 8.73 (t, *J*=5.5Hz, 1H, NH), 9.60 (d, *J*=8.0Hz, 1H, NH). ^{13}C NMR (125MHz, DMSO-d_6) δ 13.2, 18.7, 27.1, 32.4, 33.8, 37.3, 48.4, 51.4, 54.3, 55.8, 111.9, 126.5, 128.2, 129.2, 135.9, 137.3, 138.1, 143.1, 159.0, 161.7, 170.7, 172.6, 205.1. ESI-MS: *m/z* 486 ($[M+H]^+$). HRMS-ESI: calcd. for $C_{25}H_{32}N_3O_7$ 486.2240 ($[M+H]^+$), found 486.2234.

Z04. ^{1}H NMR (DMSO-d_6, 500MHz) δ 0.82 (t, *J*=7.0Hz, 3H, CH_3), 0.98-1.14 (m, 4H, CH_2), 1.19 (m, 2H, CH_2), 1.54 (m, 2H, CH_2), 2.49 (t, *J*=6.5Hz, 2H, CH_2COO), 2.70 (t, *J*=6.5Hz, 2H, $COCH_2$), 2.87 and 3.17 (m, 2H, CH_2), 3.57 (s, 3H, $COOCH_3$), 3.67 and 4.06 (m, 2H, CH_2CO), 4.00 (t, *J*=6.0Hz, 2H, NCH_2), 4.87 (m, 1H, CH), 7.20-7.37 (m, 5H, Ph), 7.43 (d, *J*=7.0Hz, 1H, C5-H in pyridinone), 8.26 (d, *J*=7.0Hz, 1H, C6-H in pyridinone), 8.74 (t, *J*=5.5Hz, 1H, NH), 9.61 (d, *J*=8.0Hz, 1H, NH). ^{13}C NMR (DMSO-d_6, 125MHz) δ 13.7, 21.8, 25.0, 27.1, 27.2, 30.4, 33.8, 37.4, 48.4, 51.3, 54.3, 56.2, 112.0 ,126.4, 128.1, 129.2, 136.2, 137.3, 138.1, 142.9, 158.9, 161.5, 170.7, 172.6, 205.1. ESI-MS: *m/z* 514 ($[M+H]^+$). HRMS-ESI: calcd. for $C_{27}H_{36}N_3O_7$ 514.2553 ($[M+H]^+$), found 514.2546.

Z05. ^{1}H NMR (DMSO-d_6, 500MHz) δ 2.50 (t, *J*=6.5Hz, 2H, CH_2COO), 2.71 (t, J= 5Hz, 2H, $COCH_2$), 2.87 and 3.18 (m, 2H, CH_2), 3.15 (s, 3H, OCH_3), 3.28-3.41 (m, 2H, OCH_2), 3.58 (s, 3H, $COOCH_3$), 3.91 and 4.20 (m, 2H, CH_2CO), 4.01(t, *J*= 6.0Hz, 2H, NCH_2), 4.88 (m, 1H, CH), 7.21-7.36 (m, 6H, Ph and buried C5-H in pyridinone), 8.03 (d, *J*=7.0Hz, 1H, C6-H in pyridinone), 8.71 (t, *J*=5.5Hz, 1H, NH), 9.62 (d, *J*=8.5Hz, 1H, NH).^{13}C NMR (DMSO-d_6, 125MHz) δ 27.1, 33.8, 37.3, 48.4, 51.4, 54.2, 55.4, 58.1, 69.7, 111.3, 126.5, 128.2, 129.1, 135.4, 137.3, 139.4, 143.2, 159.0, 162.4, 170.7, 172.6, 205.1. ESI-MS: *m/z* 488 ($[M+H]^+$). HRMS-ESI: calcd. for $C_{24}H_{30}N_3O_8$ 488.2033 ($[M+H]^+$), found 488.2023.

Z06. ^{1}H NMR (DMSO-d_6, 500MHz) δ 0.91 (d, *J*=6.5Hz, 6H, CH_3), 1.57 (m, 2H, CH_2), 1.74 (m, 1H, CH), 2.49 (t, *J*=6.5Hz, 2H, CH_2COO), 2.71 (t, *J*=6.5Hz, 2H, $COCH_2$), 3.57 (s, 3H, $COOCH_3$), 3.91-4.05 (m, 5H, NCH_3 and CH_2 in $NHCH_2CO$), 4.53 (q, *J*=7.5Hz, 1H, CH), 7.40 (d, *J*=7.0Hz, 1H, C5-H in pyridinone), 8.25 (d, *J*=7.0Hz,1H, C6-H in pyridinone), 8.58 (t, *J*=5.5Hz, 1H, NH), 9.40 (d, *J*=8.0Hz, 1H, NH). ^{13}C NMR (DMSO-d_6, 125MHz) δ 21.3, 22.9, 24.2, 27.1, 33.9, 40.4, 43.4, 48.3, 51.3, 51.5, 111.8, 136.6, 138.9, 142.9, 159.0, 161.5, 171.6, 172.6, 205.1. ESI-MS: *m/z* 410 ($[M+H]^+$). HRMS-ESI: calcd. for $C_{19}H_{28}N_3O_7$ 410.1927 ($[M+H]^+$), found 410.1917.

Z07. 1H NMR (DMSO-d_6, 500MHz) δ 0.92 (d, *J*=6.5Hz, 6H, CH_3), 1.38 (t, *J*= 7.5Hz, 3H, CH_3), 1.57 (m, 2H, CH_2), 1.73 (m, 1H, CH), 2.49 (m, 2H, CH_2COO), 2.71 (m, 2H, $COCH_2$), 3.57 (s, 3H, $COOCH_3$), 3.92-4.04(m, 2H, NCH_2), 4.19-4.34 (m, 2H, CH_2CO), 4.55 (q, *J*=7.5Hz, 1H, CH), 7.39 (d, *J*=6.5Hz, 1H, C5-H in pyridinone), 8.29 (d, *J*=6.5Hz, 1H, C6-H in pyridinone), 8.57 (t, *J*=5.5Hz, 1H, NH), 9.42 (d, *J*=8.0Hz, 1H, NH). ^{13}C NMR (DMSO-d_6, 125MHz) δ 16.5, 21.3, 23.0, 24.2, 27.1, 33.8, 40.4, 48.3, 51.4, 51.5, 51.7, 112.2, 136.0, 137.8, 142.9, 159.0, 161.8, 171.5, 172.6, 205.1. ESI-MS: *m/z* 424 ($[M+H]^+$). HRMS-ESI: calcd. for $C_{20}H_{30}N_3O_7$ 424.2084 ($[M+H]^+$), found 424.2077.

Z08. ^{1}H NMR (DMSO-d_6, 500MHz) δ 0.84 (t, *J*=7.5Hz, 3H, CH_3), 0.91 (d, *J*=6.5Hz, 6H, CH_3), 1.24 (m, 2H, CH_2), 1.57 (m, 2H, CH_2), 1.74 (m, 3H, CH_2CH), 2.49 (t, *J*=6.5Hz, 2H, CH_2COO), 2.72 (t, *J*=6.5Hz, 2H, $COCH_2$), 3.57 (s, 3H, $COOCH_3$), 3.91-4.02 (m, 2H, NCH_2), 4.15-4.32 (m, 2H, CH_2CO), 4.54 (q, *J*=7.0Hz, 1H, CH), 7.43 (d, *J*=7.0Hz, 1H, C5-H in pyridinone), 8.32 (d, *J*=7.0Hz, 1H, C6-H in pyridinone), 8.60 (t, *J*=6.0Hz, 1H, NH), 9.45 (d, *J*=8.0Hz, 1H, NH).^{13}C NMR (DMSO-d_6, 125MHz) δ 13.2, 18.9, 21.2, 22.9, 24.1, 27.1, 32.7, 33.8, 40.4, 48.3, 51.3, 51.5, 56.1, 112.0, 136.3, 138.2, 143.0, 158.9, 161.6, 171.5, 172.6, 205.0. ESI-MS: *m/z* 452 ($[M+H]^+$). HRMS-ESI: calcd. for $C_{22}H_{34}N_3O_7$ 452.2397 ($[M+H]^+$), found 452.2392.

Z09. ^{1}H NMR(DMSO-d_6, 500MHz) δ 0.84 (t, *J*=6.5Hz, 3H, CH_3), 0.91 (d, *J*=6.5Hz, 6H, CH_3), 1.22 (m, 6H, CH_2), 1.57 (m, 2H, CH_2), 1.70-1.80 (m, 3H, CH_2CH), 2.49 (t, *J*=6.5Hz, 2H, CH_2COO), 2.71 (t, J=6.5Hz, 2H, $COCH_2$), 3.57 (s, 3H, $COOCH_3$), 3.91-4.03(m, 2H, NCH_2), 4.14-4.32 (m, 2H, CH_2CO), 4.55 (q, *J*=7.0Hz, 1H, CH), 7.44 (d, *J*=7.0Hz, 1H, C5-H in pyridinone), 8.32 (d, *J*=7.0Hz, 1H, C6-H in pyridinone), 8.60 (t, *J*=6.0Hz, 1H, NH), 9.46 (d, *J*=7.5Hz, 1H, NH). ^{13}C NMR (DMSO-d_6, 125MHz) δ 13.7, 21.3, 21.9, 22.9, 24.2, 25.2, 27.1, 30.6, 30.7, 33.8, 40.4, 48.3, 51.3, 51.5, 56.3, 112.0, 136.3, 138.2, 143.0, 158.9, 161.5, 171.5, 172.5, 205.0. ESI-MS:

m/z 480 ([M+H]$^+$). HRMS-ESI: calcd. for $C_{24}H_{38}N_3O_7$ 480.2710 ([M+H]$^+$), found 480.2701.

Z10. ^{1}H NMR (DMSO-d_6, 500MHz) δ 0.92 (d, *J*= 6.0Hz, 6H, CH_3), 1.59 (m, 2H, CH_2), 1.76 (m, 1H, CH), 2.51 (t, *J*=6.5Hz, 2H, CH_2COO), 2.73 (m, 2H, $COCH_2$), 3.23 (s, 3H, OCH_3), 3.58 (s, 3H, $COOCH_3$), 3.60-3.73 (m, 2H, OCH_2), 3.93-4.05 (m, 2H, NCH_2), 4.39 (m, 1H, CH), 4.50 (m, 2H, CH_2CO), 7.34 (d, *J*=6.5Hz, 1H, C5-H in pyridinone), 8.12 (d, *J*=6.5Hz, 1H, C6-H in pyridinone), 7.91 (t, *J*=5.5Hz, 1H, NH), 8.81 (d, *J*=8.0Hz, 1H, NH). ^{13}C NMR (DMSO-d_6, 125MHz) δ 21.2, 23.0, 24.2, 27.1, 33.8, 40.2, 48.3, 51.3, 51.7, 55.5, 58.1, 70.0, 111.4, 135.4, 139.4, 143.2, 159.1, 162.7, 171.6, 172.6, 205.1. ESI-MS: *m/z* 454 ([M+H]$^+$). HRMS-ESI: calcd. for $C_{21}H_{32}N_3O_8$ 454.2189 ([M+H]$^+$), found 454.2182.

3.2. Biological assay

3.2.1. Cell Culture

The biological evaluation for ALA, ALA in combination with CP94 as a mixture and ten novel ALA-HPO conjugates were carried out in a range of human cell lines. A549 cell line (human lung carcinoma), MDA MB-435 and MCF-7 cell lines (human breast adenocarcinoma), and Hela cell line (human cervical cells) were cultured in Dulbecco's Modified Eagle Medium media (DMEM). Human mouth epidermal carcinoma cell (KB cell line) was cultured in Eagle's minimum essential medium (EMEM). Human prostate cells derived from metastatic site lymph node (LNCap cell line) and normal human prostate epithelial cell (BPH-1 cell line) were both cultured in Roswell Park Memorial Institute (RPMI 1460). All types of media contained L-glutamine (20 μM) and phenol red, supplemented with 10% fetal bovine serum (FBS) and Gentamycine (500 units/mL; Life Technologies). They were standardized to give an iron concentration between 450 and 600 μg/100 g. The cells were grown as monolayers in sterile, vented-capped, angle-necked cell culture flasks (Corning) and were maintained at 37 °C in a humidified 5% CO_2 incubator (IR Autoflow Water-Jacketed Incubator; Jencons Nuaire) until confluent.

3.2.2. Fluorescence Pharmacokinetics

Cells were seeded into gama-sterilised 96 well plates (Orange Scientific, Triple Red Laboratory Technologies) at a density of approximately 5×10^4 cells per well for 48 hours. After removing the culture medium, the wells were washed with PBS. The cells were incubated with freshly prepared solutions of ALA and ALA-HPO prodrugs: 100μL of serum-free medium containing 5% DMSO and varying prodrug concentrations was added to a designated series of wells. Each plate contained control wells with cells without prodrug for determination of the background reading, and reference wells containing cells incubated with the same ALA concentrations. For drug incubation, serum-free medium was used since serum is known to cause release of PpIX from cells, thus resulting in loss of the florescence signal. The fluorescence signal from each well was measured with a fluorescence spectrometer plate reader using 405 nm excitation and 635 nm emission wavelengths, with slit widths set to 10 nm and an internal 515 nm long-pass filter on the emission side. The spectral scans were recorded between 600 and 750 nm, thereby selectively identifying PpIX. The mean fluorescence intensity (expressed in arbitrary units) was calculated after subtraction of the control values. PpIX fluorescence intensities were recorded over periods of 3, 6, and 24 h with varied concentration of ALA prodrugs (50–250 μM).

3.2.3. Photodynamic Treatment

Cells were seeded into 96-well plates at a density of approximately 5×10^4 per well. Following incubation for 48h, the cells were washed with PBS and 100μL solutions containing each compound at varying concentrations (between 50μM–250 μM) were added to their designated wells for 4h incubation periods. Each well plate contained three control wells without the compound and the compound at five different concentrations in triplicate. The plates were irradiated with a fluence of (5 min) using a blue lamp, which emits a uniform field. Peak output is 420 nm, which overlaps with the PpIX soret band. Immediately following irradiation, the medium was replaced and cells were incubated for further 18h. Cell cytotoxicity was determined using the 3-(4,5-dimethylthiazol-2-yl)-2,5-diphenyltetrazolium bromide (MTT) assay: The cells were incubated with the compounds for 4h, washed, and after 18h they were subjected to the MTT assay. Cells were incubated with medium containing MTT (1mg/mL dissolved in full media) for 2h. The insoluble end product (formazan derivatives) was dissolved in 100 μL DMSO after removing the medium. UV absorption was quantified at 490 nm using a 96-well plate reader (MR 700 Dynatech, Dynex). The mean cell survival was calculated for each prodrug at every concentration tested and expressed as a percentage of control (cells only without the compounds but irradiated) cell survival values. For determination of "dark" toxicity of the compounds, well plates were prepared in the same manner as above but without irradiation.

4. Conclusions

Although ALA is a useful therapeutical agent for PDT, it is important to improve its bioavailability when administered systemically and intravenously in order to overcome distribution problems. Incorporation of iron chelating agents to ALA prodrugs offers a promising way to enhance the cellular PpIX accumulation by inhibiting ferrochelatase. In the present study, a series of ALA–HPO conjugates have been synthesized. Among these ALA prodrugs, **Z01** exhibited the highest efficiency in cellular PpIX accumulation in a range of cell lines. **Z01** was also found to be the most effective in enhancement of tumor cell phototoxicity when compared to ALA and to a combination of ALA with CP94. It is necessary to extend these promising results in an in vivo setting in order to further evaluate the potential of these ALA–HPO conjugates.

Acknowledgments

The authors thank Science Technology Departmentof Zhejiang Province, China (No. 2013C24006) and Zhejiang Provincial Natural Science Foundationof China (No. LY12B02014) for the financial support and ChemPharm Research LTD, UK. We also acknowledge the assistance in the measurement of some of the efficacy studies by Dr. Olivier Reefs at Department of Pharmacy and Pharmacology, Bath University, UK.

Notes and references

1 M. Ochsner, *J. Photochem. Photobiol.*, 1997, **39**, 1–18.
2 G. B. Snow and G. A. van Dongen, *Anticancer Res.*, 2003, **23**, 505–522.
3 A. Juzeniene, Q. Peng and J. Moan, *Photochem. Photobiol. Sci.*, 2007, **6**, 1234–1245.
4 S. Q. Tao, F. Li, L. Cao, R. S. Xia, H. Fan, Y. Fan, H. Sun, C. Jing and L. J. Yang, *Cell Biochem. Biophy.*, 2015, **73**, 701–706.
5 E. W. Jeffes, J. L. McCullough, G. D. Weinstein, P. E. Fergin, J. S. Nelson, T. F. Shull, K. R. Simpson, L. M. Bukaty, W. L. Hoffman and N. L. Fong, *Arch. Dermatol.*, 1997, **133**, 727–732.
6 T. Hasegawa, Y. Suga, Y. Mizuno, K. Haruna, H. Ogawa and S. Ikeda, *J. Dermatol.*, 2010, **37**, 623–628.
7 T. Dai, Y. Y. Huang and M. R. Hamblin, *Photodiagn. Photodyn. Ther.*, 2009, **6**, 170–188.
8 O. E.Akilov, S.Kosaka, K.O'Riordan and T. Hasan, *Photochem. Photobiol. Sci.*, 2007, **6**, 1067–1075.
9 A. Stenzl, H. Penkoff, E. Dajc-Sommerer, A. Zumbraegel, L. Hoeltl, M. Scholz, C. Riedl, J. Bugelnig, A. Hobisch, M. Burger, G. Mikuz and U. Pichlmeier, *Cancer*, 2011, **117**, 938–947.
10 R. F. V. Lopez, N. Lange, R. Guy and M. V. L. B. Bentley, *Adv. Drug Deliv. Rev.,* 2004, **56**, 77–94.
11 Q. Peng, K. Berg, J. Moan, M. Kongshaug and J. M. Nesland, *Photochem. Photobiol.*, 1997, **65**, 235–251.
12 J. H. Yoon, H. E. Yoon, O. Kim, S. K. Kim, S. G. Ahn and K. W. Kang, *Lasers Surg. Med.*, 2012, **44**, 76–86.
13 C. J. Whitaker, S. H. Battah, M. J. Forsyth, C. Edwards, R. W. Boyle and E. K. Matthews, *Anti-Cancer Drug Des.*, 2000, **15**, 161–170.
14 F. Giuntini, L. Bourre, A. J. MacRobert, M. Wilson and I. M. Eggleston, *J. Med. Chem.*, 2009, **52**, 4026–4037.
15 G. Di Venosa, P. Vallecorsa, F. Giuntini, L. Mamone, A. Batlle, S. Vanzuli, A. Juarranz, A. J. MacRobert, I. M. Eggleston and A. Casas, *Mol. Cancer Ther.*, 2015, **14**, 440–451.
16 Q. Peng, T. Warloe, K. Berg, J. Moan, M. Kongshaug, K. E. Giercksky and J. M. Nesland, *Cancer*, 1997, **79**, 2282–2308.
17 J. Kloek, W. Akkermans and G. M. Beijersbergen van Henegouwen, *Photochem. Photobiol.*, 1998, **67**, 150–154.
18 B. Krammer and K. Plaetzer, *Photochem. Photobiol. Sci.*, 2008, **7**, 283–289.
19 L. Teng, M. Nakada and S. G. Zhao, *Br. J. Cancer*, 2011, **104**,798–807.
20 H. Fukuhara MD, K. Inoue, A. Kurabayashi, M. Furihata, H. Fujita, K. Utsumi, J. Sasaki and T. Shuin, *Photodiagn. Photodyn. Ther.*, 2013, **10**, 399–409.
21 J. Hanania and Z. Malik, *Cancer Lett.*, 1992, **65**, 127–131.
22 J. B. Yang, Y. M. Xia, X. M. Liu, S. Jiang and L. Y. Xiong, *Laser Med. Sci.*, 2010, **25**, 251–257.
23 K. Choudry, R. C. C. Brooke, W. Farrar and L. E. Rhodes, *Br. J. Dermatol., 2003,* 149, 124-130.
24 S. Fijan, H. Honigsmann, B. Orte, *Br. J. Dermatol.*, 1995, **133**, 282–288.
25 S. C. Chang, A. J. MacRobert, J. B. Porter, S. G. Bown, *J. Photochem. Photobiol. B*, 1997, **38**, 114–122.
26 A. Curnow, B. W. Mcllroy, M. J. Postle-Hacon, J. B. Porter, A. J. MacRobert and S. G. Bown, *Br. J. Cancer*, 1998, **78**, 1278–1282.
27 E. Blake, J. Allen and A. Curnow, *Photochem. Photobiol.*, 2011, **87**, 1419–1426.
28 E. Blake and A. Curnow, *Photochem. Photobiol.*, 2010, **86**, 1154–1160.
29 C. F. Zhu, S. Battah, X. L. Kong, B. J. Reeder, R. C. Hider and T. Zhou, *Bioorg. Med. Chem. Lett.*, 2015, **25**, 558–561.
30 S. Basavaraj, G. V. Betageri, *Acta Pharm. Sinica B*, 2014, **4**, 3–17.
31 http://www.molinspiration.com/cgi-bin/properties.
32 F. S. De Rosa, R. F. V. Lopez, J. A. Thomazine, A. C. Tedesco, N. Lange and M. V. L. B. Bentley, *Pharm. Res.*, 2004, **21**, 2247–2252.
33 F. S. De Rosa, A. C. Tedesco, R. F. V. Lopez, M. B. Pierre, N. Lange, J. M. Marchetti, J. C. Rotta and M. V. L. B. Bentley, *J. Control. Release*, 2003, **89**, 261–269.
34 J. R. W. Masters, *Nat. Rev. Cancer*, 2010, **10**, 441-448.